INFLUENCE OF CRACK DENSITY ON THE HYDRO-MECHANICAL BEHAVIOR OF A HORIZONTAL BOREHOLE UNDER ISOTROPIC COMPRESSIVE STRESS

Nguyen Thi Thu Nga[1,*], Tran Nam Hung[1]
[1]*Le Quy Don Technical University*

Abstract

The excavation of boreholes induces a damage zone in the vicinity of the boreholes, and thereby affects the hydro-mechanical properties of the rock mass surrounding. This paper outlines analytical models of effective permeability and moduli of the porous rock containing a randomly crack distribution, which is an explicit function of the dimensionless crack density, crack conductivity, crack length and matrix permeability. These proposed models are then introduced into a finite element open source code, Code_Aster, to study hydro-mechanical responses of the medium around a horizontal borehole under isotropic far-field compressive stress for different cases of crack density. The results showed that the crack density changes the effective permeability and moduli and therefore under isotropic compressive stress it influences significantly the behavior of the borehole.

Keywords: *Effective permeability; horizontal borehole; hydro-mechanical behavior; porous medium; crack density.*

1. Introduction

Boreholes are widely used for many different purposes including the extraction of water, liquids or gases or for underground storage of unwanted substances, for example in carbon capture and storage. They are bored in the ground, either vertically or horizontally [1-3].

Most underground works such as drifts, drilling, mining, etc., causes damage for the rock mass in the vicinity of the openings due to the excavation, i.e. damaged zone. This damage modifies the hydro-mechanical properties of the rock, in particularly, the change of permeability that had been shown by experimental studies [4-7]. Therefore, the deep understanding on the hydro-mechanical coupling of the damaged zone around the opening is one of interesting eco-scientific subjects to reduce the cost of the underground works including boreholes.

In geo-mechanical engineering applications, geo-materials are normally saturated with one or several phases of fluid and generally heterogeneous with different fracture families. In the literature, the permeability of the fractured zone is usually assumed to be

* Email: nguyennga@lqdtu.edu.vn
https://doi.org/10.56651/lqdtu.jst.v3.n01.71.sce

constant in large scale geo-mechanical application [9-11]. Moreover, the evolution of mechanical properties and permeability is normally uncoupled by numerical approaches [12, 13], by empirical and statistical investigations [14] or by homogenization technique [15-17]. However, cracking considerably increased the permeability because under compressive stress, the cracks tend to grow and coalesce to form a percolated network [8]. Thus, a coupled hydro-mechanical model of the rock taking into account the effects of the change of the permeability is essential in simulating the response of the boreholes.

Recently, an analytical model describing the physical behavior of fluid flow through a cracked porous material was proposed (see [18, 19]). According to these researches, the fluid flow obeys Poisseuille's law along the crack and Darcy's law in the porous medium. Flow through and around a single crack are explicitly derived, which is an important key for estimation of effective permeability. In the present study, this model is incorporated in the open source finite element code (Code_Aster) to study the hydro-mechanical responses of the excavation induced damaged zone (EDZ) around a horizontal borehole. The crack density in this zone depends on the mechanical properties of host rock. Therefore, different crack densities are considered to show their effect on the hydro-mechanical behavior of the rock mass around the borehole.

2. Effective Permeability of Porous Medium

Let us consider a heterogeneous permeable medium occupying a domain Ω in space, containing a crack network Γ. As shown in [20], the average of Darcy's velocity reads:

$$\bar{v} = -\boldsymbol{k}^{eff}.\bar{G} = \frac{1}{\Omega}\left[\int_{\Omega} v d\omega + \sum_{m}\int_{\Gamma_m} qds\right] \tag{1}$$

where $\bar{G} = \frac{1}{\Omega}\int_{\Omega} p(x).n(x)d\Omega$ is the average pressure gradient within Ω, $q(x)$ is Darcy's velocity at point x, $p(x) = A.x$ is a pressure of fissure on its boundary and $A = \frac{1}{\Omega}\int_{\Omega}\nabla p d\omega$ is a constant pressure gradient.

As seen in (1), $\frac{1}{\Omega}\int_{\Omega} v d\omega = -\mathbb{k}.A$ presented the flow occurred in the porous medium following Darcy's law and $\frac{1}{\Omega}\sum_{m}\int_{\Gamma_m} qds = -\mathbb{k}^f A$ related to the global contribution of the fractures to the flow in the domain. Therefore, the effective permeability $\boldsymbol{k}^{eff}$ of an elastic porous medium taken from the dilute model can be written as:

$$\mathbb{k}^{eff} = \mathbb{k} + \mathbb{k}^{f} \tag{2}$$

where $\mathbb{k}$ is the permeability tensor of solid medium (without pores) and $\mathbb{k}^{f}$ is the permeability tensor in factures.

Recall that the fluid flow along the crack obeys Poisseuille's law and Pouya and Vu (2012) (see in [21]) obtained an analytical solution for the integral of fluid flow over the crack as in the following:

$$\frac{1}{\Omega}\sum_{m}\int_{\Gamma_m} q ds = \frac{1}{\Omega}\frac{2\pi c L^2\sqrt{|\mathbb{k}|}}{2c+\pi L\sqrt{|\mathbb{k}|}}(t\otimes t)A \tag{3}$$

in which *c, L, t* being the crack hydraulic conductivity, the halt-length of crack and the tangential vector to crack defining its orientation, respectively.

The relationship between the crack hydraulic conductivity and the crack aperture *e* in can be read by mean of a cubic law [22, 23]:

$$c = \gamma g \frac{e^3}{12 f \mu} \tag{4}$$

where γ, g, f, μ are respectively the fluid density, the gravity, the friction factor accounting for the fracture roughness (fracture spacing) and the fluid dynamic viscosity.

It is noted that the definition of permeability of the crack family is:

$$k = \frac{c}{e} \tag{5}$$

Now we consider a crack family which has N cracks, characterized by an average length 2L, an average orientation *t*, a density $\rho = \frac{N}{\Omega}$. The cracks are supposed to have no interaction between them. The effective permeability of all cracks was derived using self-consistent scheme [18]:

$$\mathbb{k}^{f} = \frac{N}{\Omega}\frac{2\pi c L^2\sqrt{|\mathbb{k}^{eff}|}}{2c+\pi L\sqrt{|\mathbb{k}^{eff}|}}(t\otimes t) \tag{6}$$

The crack density is defined as:

$$\bar{\rho} = \frac{N}{\Omega}\pi L^2 = \rho\pi L^2 \tag{7}$$

Introducing the definition of $\bar{\rho}$ in Eq. (6) then substituting Eq. (6) into Eq. (2), the effective permeability for this medium can be rewritten as follows:

$$\mathbb{k}^{eff} = \mathbb{k} + \frac{2c\bar{\rho}\sqrt{\left|\mathbb{k}^{eff}\right|}}{2c + \pi L\sqrt{\left|\mathbb{k}^{eff}\right|}}(t \otimes t) \tag{8}$$

In case of a random distribution of equal size cracks, the average of $(t \otimes t)$ is equal to $\frac{1}{2}\delta$ with δ unit tensor. Consequently, the effective permeability tensor is isotropic with the diagonal component:

$$k^{eff} = k\frac{c\bar{\rho}\sqrt{\left|k^{eff}\right|}}{2c + \pi L\sqrt{\left|k^{eff}\right|}} \tag{9}$$

The Eq. (9) is a quadratic equation and has a simple root:

$$k^{eff} = k\left[\frac{1}{2} + \frac{(\bar{\rho}-2)\eta}{2\pi} + \frac{\eta}{2\pi}\sqrt{\frac{8\pi}{\eta} + \left(2 - \bar{\rho} - \frac{\pi}{\eta}\right)^2}\right] \tag{10}$$

where $\eta = \dfrac{c}{kL}$ is the dimensionless fracture hydraulic conductivity.

Therefore, the dimensionless hydraulic conductivity can be written as:

$$\frac{k^{eff}}{k} = \left[\frac{1}{2} + \frac{(\bar{\rho}-2)\eta}{2\pi} + \frac{\eta}{2\pi}\sqrt{\frac{8\pi}{\eta} + \left(2 - \bar{\rho} - \frac{\pi}{\eta}\right)^2}\right] \tag{11}$$

As observed in Eq. (9), the dimensionless hydraulic conductivity depends on fracture hydraulic conductivity and crack density (i.e., $\dfrac{k^{eff}}{k} = f(\bar{\rho}, \eta)$). It should be noted that both $\bar{\rho}$ and η depend on the length of crack which has a propagation under stress. Thus, the permeability changes due to crack growth and stress that has been proved in [24].

3. Effective Moduli of Porous Medium

Considering a saturated medium with linear elastic solid containing cracks of diverse shapes and arbitrary orientation distributions. Two types of shapes: needle-shaped spheroidal cavity or crack-like spheroidal cavity filled with non-viscous compressible fluid (which is characterized by the fluid compressibility κ) are considered in the study of Shafiro and Kachanov [25]. Taking into account the stress interactions between the cracks in analyzing in terms of elastic potentials, the effective compliance tensor $\mathbb{S}$ is written in the form:

$$\mathbb{S}=\begin{pmatrix} \frac{1}{E_1} & -\frac{\nu_{12}}{E_1} & -\frac{\nu_{13}}{E_1} & 0 & 0 & 0 \\ -\frac{\nu_{21}}{E_2} & \frac{1}{E_2} & -\frac{\nu_{23}}{E_2} & 0 & 0 & 0 \\ -\frac{\nu_{31}}{E_3} & -\frac{\nu_{32}}{E_3} & \frac{1}{E_3} & 0 & 0 & 0 \\ 0 & 0 & 0 & \frac{1}{\mu_{23}} & 0 & 0 \\ 0 & 0 & 0 & 0 & \frac{1}{\mu_{31}} & 0 \\ 0 & 0 & 0 & 0 & 0 & \frac{1}{\mu_{12}} \end{pmatrix} \tag{12}$$

The effective elastic properties are best analyzed in terms of elastic potentials in stresses: $f = f_0 + \Delta f$ where f, $f_0, \Delta f$ are respectively the total potential, the potential in absence of cavities and the potential due to cavities.

For an isotropic crack distribution, the components of (12) can be defined as follows:

$$\begin{aligned} &E_1 = E_2 = E_3 = E,\ \mu_{31} = \mu_{23} = \mu_{12} = \mu,\ \nu_{12} = \nu_{23} = \nu_{31} = \nu \\ &\frac{E_0}{E} = 1 + \frac{16}{45}\frac{(1-\nu_0^2)}{(2-\nu_0)}\left[(10-3\nu_0)\zeta - 3(2-\nu_0)\zeta_1\right] \\ &\frac{\mu_0}{\mu} = 1 + \frac{16}{45}\frac{(1-\nu_0)}{(2-\nu_0)}\left[(5-\nu_0)\zeta - (2-\nu_0)\zeta_1\right] \end{aligned} \tag{13}$$

where

$$\zeta = \frac{1}{\Omega}\sum_{i=1}^{n}(L^2)^{(i)},\quad \zeta_1 = \frac{1}{\Omega}\sum_{i=1}^{n}\left(\frac{L^2}{1+\delta_c}\right)^{(i)},\quad \delta_c = \gamma\frac{\pi}{4(1-\nu_0^2)}\left[\kappa E_0 - 3(1-2\nu_0)\right] \tag{14}$$

E_0, μ_0 and ν_0 are the Young's moduli, the shear moduli and the Poisson's ratios of uncracked medium, respectively; $\gamma = e/L < 1$ is aspect ratio of cracks; n is number of crack families. For more details, the reader could see in [26].

4. Numerical Test

We consider a horizontal borehole of radius r_0 = 0,1m excavated in an isotropic saturated porous medium whose poro-elastic properties are taken as follows: Young's modulus: $E_{0x} = E_{0y} = 5600$ MPa, the Poisson's ratios: $\nu_{0xz} = \nu_{0yz} = 0{,}14$ and the shear modulus: $\mu_{0xy} = \dfrac{E_0}{2(1+\upsilon_0)} = 2456$ MPa. This borehole drilled in the medium subjected to a uniform pore pressure $p^{ff} = 4{,}7$ MPa, the initial stresses $\sigma_{vff} = \sigma_{hff} = 12{,}5$ MPa at far-field as well as the mud pressure $p_W = 10$ MPa on the borehole boundary [9].

Due to the symmetry of the considered problem, only one quarter of the model is considered as shown in Fig. 1. Note that $\kappa = \dfrac{1}{2200}(\dfrac{1}{\text{MPa}})$ for the water. Considering the Beishan granite [19], the crack aperture and the isotropic permeability of the uncracked medium are $e = 1{,}73\times10^{-6}$ (m) and $k_x = k_y = k = 2{,}0\times10^{-20}$ (m^2). The crack density $\bar{\rho}$ is supposed to be from 1,0 to 5,0 while the half-length of crack L is 0,00012 (m).

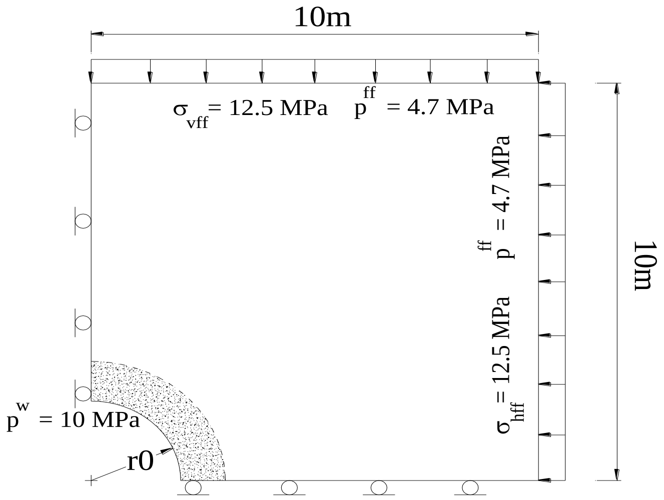

Figure 1. The finite element simulation of the borehole in 2D plane strain by Code_Aster.

According to the relations (14), (13) and (11), the others parameters of the damaged zone are presented in Tab. 1. Size of EDZ depends on the rock properties, the initial stresses and the axcavation rate. In this study, we suppose that EDZ distributes around the opening in the range of a half of the radius r_0 from the borehole boundary.

To study the hydro-mechanical behavior of the borehole and EDZ around it, the finite element open source code Code_Aster is used. Code_Aster is the software on which we can include material parameters as functions that can be established using

Python language, which can be embedded into source code of the software. Thus, the effective permeability as well as the effective elastic constants of EDZ can be calculated directly in Code_Aster.

The analyses of stress-strain state in both cases of impermeable and permeable rocks are considered. Depending on the hydraulic boundary condition on the borehole wall, the mud pressure p_W can act both as a radial stress and as a pore pressure (case of permeable boundary) or act only as a radial stress (case of impermeable boundary). We note p_0 as the pore pressure on the borehole wall which will be equal to p^{ff} ($p_0 = p^{ff}$) in the impermeable boundary case or equal to p_W ($p_0 = p_W$) in the permeable boundary case.

For each case, four different crack density $\bar{\rho}$ of 0,0; 1,0; 2,0 and 5,0 were designed and labeled as CAS0, CAS1, CAS2, and CAS3, respectively. The material properties are shown in Tab. 1.

Table 1. Parameters of damaged zone around the borehole

Cases / Parameters	$\bar{\rho}=1,0$	$\bar{\rho}=2,0$	$\bar{\rho}=5,0$
δ_c	0,0044	0,0044	0,0044
η	299636	299636	299636
ζ	0,318	0,636	1,591
ζ_1	0,317	0,633	1,584
E (MPa)	4516	3783	2544
μ (MPa)	2122	1868	1374
k^{eff} (m^2)	$4,0\times10^{-20}$	$874,7\times10^{-20}$	572557×10^{-20}

It is noted that the behavior of borehole under isotropic compressive stress is also isotropic. In general, we can see the difference between the impermeable case and permeability case in the rock. Fig. 2 presents the results of radial displacement on the boundary of the borehole for four cases of $\bar{\rho}$ to point out differences between the permeable and impermeable cases. In case of impermeability, no difference can be observed by time, from 1 hour to 2 days for each case of crack density. On the contrary, the permeable case shows that the radial displacement of the wellbore wall increases over time and it attains stability value after short time (the line for t = 1 day coincides with the one for 2 days, see Fig. 3b). In addition, in Fig. 3, the radial displacement in the permeable case are considerably higher than that of impermeable case when the crack density increases. The comparison between displacements at 1 hour and at 2 days shows a maximum difference about 58% and 108% for the impermeable and permeable cases, respectively.

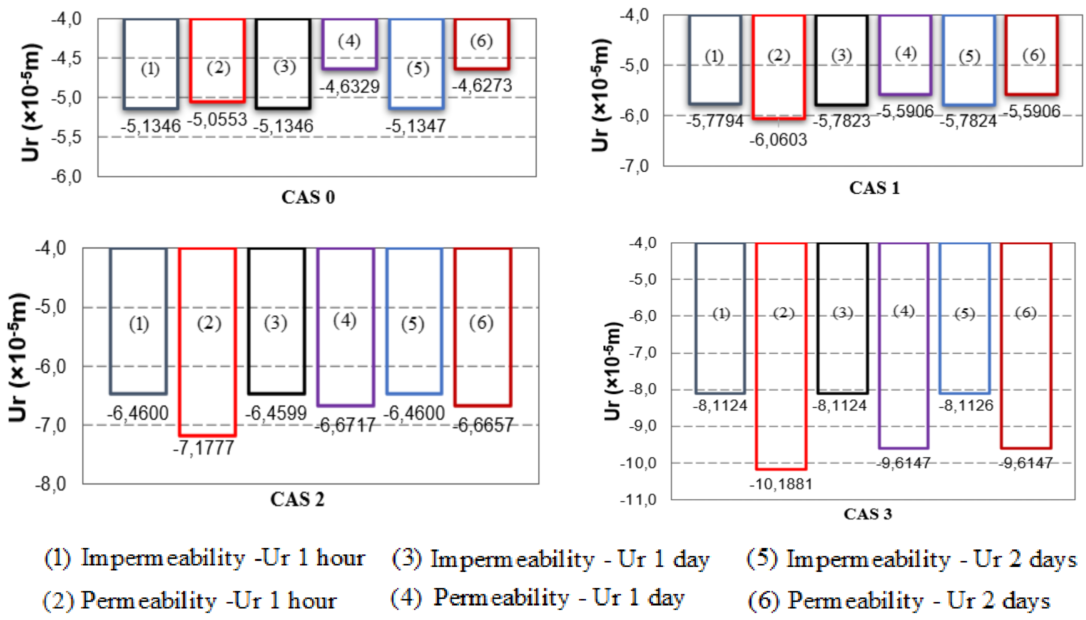

Figure 2. Radial displacement Ur on the borehole boundary: Comparison between the permeable and impermeable cases and for 4 cases of crack density.

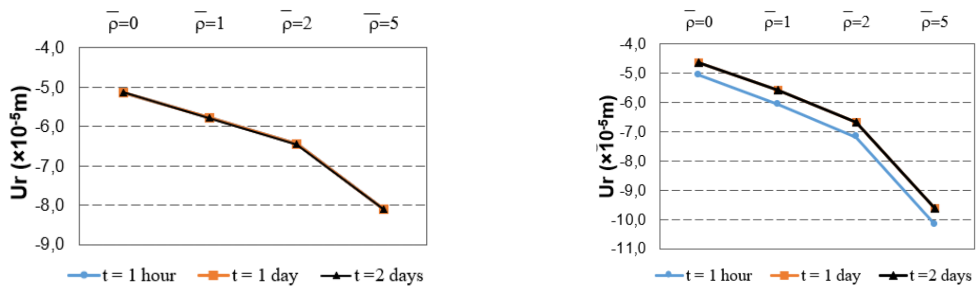

(a) Impermeable case *(b) Permeable case*

Figure 3. Evolution of the radial displacement Ur calculated from the impermeable and permeable cases for four cases of crack density.

Figure 4 presents the results of tangential stress on the borehole boundary (hoop stress) calculated from the numerical simulation at different instants of time from 1 hour to 2 days for two state of permeability. In general, we can state that the hoop stress is time-independent and can be considered constant in function of crack density. The impermeable state gives stress values higher than the permeable state with the differences from 4,5% to 5,7%.

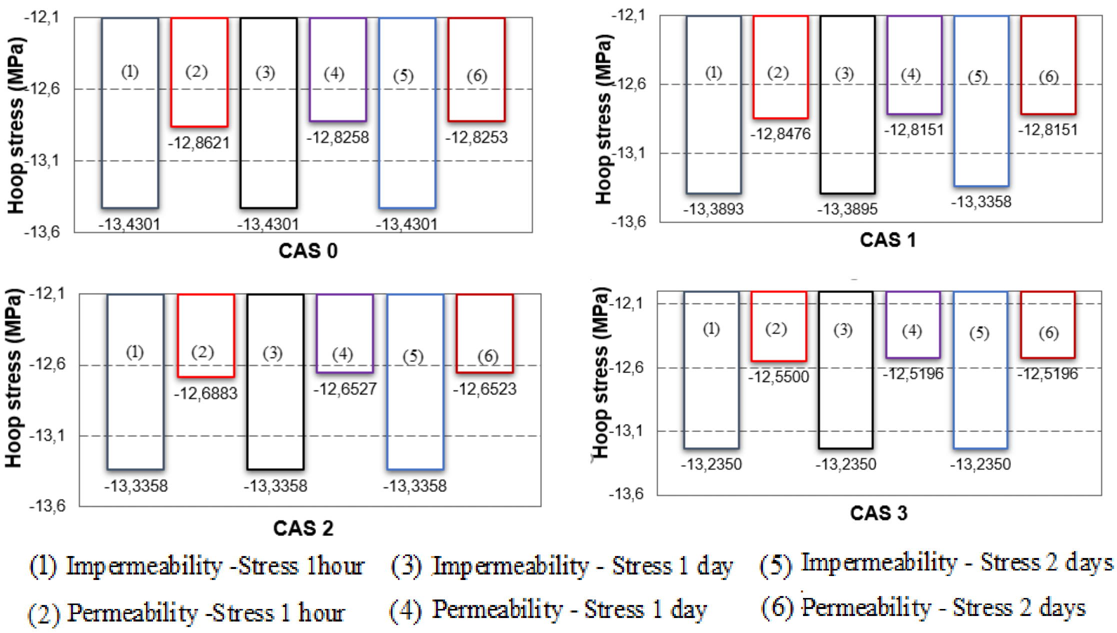

Figure 4. The hoop stress (MPa) on the borehole boundary: Comparison between the permeable and impermeable cases and for 4 cases of crack density.

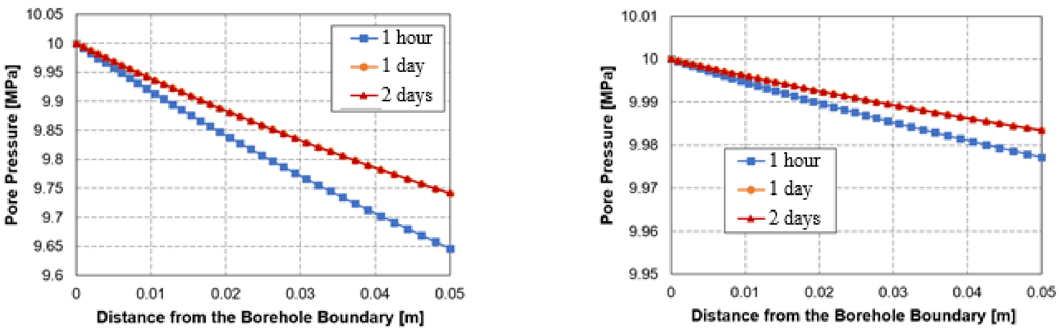

CAS1 **CAS3**

Figure 5. Pore pressure evolution in EDZ for CAS1 and CAS3.

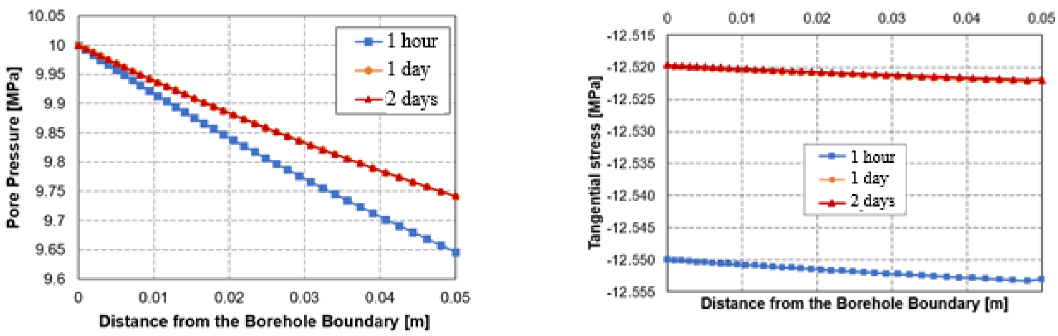

CAS1 **CAS3**

Figure 6. Tangential stress evolution in EDZ for CAS1 and CAS3.

Figure 5 and Figure 6 present the evolution of the pore pressure and tangential stress in EDZ over time. It can be seen that the pore pressure in EDZ attends stable value (note that the line for 1 day coincides with the line for 2 days) after one day for both CAS1 and CAS3. This is also the case of tangential stress illustrated in Fig. 6. It is observed that the differences of pore pressure and tangential stress between the borehole wall and the EDZ boundary is higher in CAS1 corresponding to the smaller crack density.

5. Conclusion

In this study, the theoretical models of effective permeability and moduli are outlined for the excavation induced damaged zone around a horizontal borehole and then are implemented in open source finite element code to study the hydro-mechanical behavior of the borehole.

The results show that under isotropic compressive stress, the effective permeability and moduli of the rock in the vicinity of the borehole change remarkably the behavior of the borehole where the stress reduces and displacement increases. This suggests that it is necessary to take into account the effective permeability and moduli of the rock surrounding the opening to evaluate the stability of the borehole.

Future work will devote to study a horizontal borehole in anisotropic permeable rock taking into account an anisotropic crack distribution with crack growth which could be considered a right perspective.

Acknowledgment

This research is funded by Vietnam National Foundation for Science and Technology Development (NAFOSTED) under grant number 107.01-2017.307.

References

1. Do, D.P., Tran, N.H, & Hoxha, D. (2017). Behavior of horizontal borehole in anisotropic poroelastic media with transient fluid flow: a closed-form solution based on the complex potential approach. *Poromechanics VI, Paris,* 9-13 July.
2. Yan, J., Zili, Q., Mian,C., Fuxiang, Z., & Yunhu, L. (2013). Study on mechanisms of borehole instability in naturally fractured reservoir during production test for horizontal wells. *Pet Sci Technol*, *31*, pp. 829-839.
3. Qin, W., Xu, J., Hu, G., Gao, J., & Xu, G. (2019). Measurement and simulation study on effective drainage radius of borehole along coal seam. *Energy Exploration & Exploitation*, *37*(6), pp. 1657-1679.
4. Oda, M., Takemura, T., & Aoki, T. (2002). Damage growth and permeability change in triaxial compression tests of Inada granite, *Mechanics of Materials, 34*(6), pp. 313-331.

5. Chen,Y., Hu, S., Wei, K., Hu, R., Zhou, C., & Jing, L. (2014). Experimental characterization and micromechanical modeling of damage-induced permeability variation in Beishan granite. *International Journal of Rock Mechanics and Mining Sciences, 71*, pp. 64-76.
6. Wang, J.A., Park, H. D. (2002). Fluid permeability of sedimentary rocks in a complete stress-strain process. *Engineering Geology*, *63*(3-4), pp. 291-300.
7. Bossart, P., Meier , P. M., Moeri, A., Trick, T.,& Mayor, JC. (2002). Geological and hydraulic characterisation of the excavation disturbed zone in the Opalinus Clay of the Mont Terri Rock Laboratory. *Engineering Geology*, *66*(1-2), pp. 19-38.
8. Rayhani, M. H., Yanful, E. K. & Fakher, A. (2012). *Desiccation-induced cracking and its effect on the M.N. Vu. Modélisation des écoulements dans des milieux poreux fractures par la méthode des équations intégrales singulières*. PhD thesis, Ecole des Ponts ParisTech, France, in French.
9. Do, D. P., Tran, N. H., Dang, H. L. & Hoxha, D. (2019). Closed-form solution of stress state and stability analysis of wellbore in anisotropic permeable rocks. *International Journal of Rock Mechanics and Mining Sciences, 113*, pp. 11-23.
10. Tran, N.H., Do, D.P., & Hoxha, D. (2018). A closed-form hydro-mechanical solution for deep tunnels in elastic anisotropic rock. *European Journal of Environmental and Civil Engineering 22*(12), pp. 1429-1445.
11. Seyedi, D., Ducellier, A., Vu, M.N., & Pouya, A. (2011). A two-scale model for simulating the hydromechanical behavior of faults during CO_2 geological storage operation. *In: 45th U.S. Rock Mechanics / Geomechanics Symposium.* San Francisco, California; 26-29 June.
12. Nguyen, T.K., Pouya, A., & Rohmer, J. (2015). Integrating damage zone heterogeneities based on stochastic realizations of fracture networks for fault stability analysis. *Int. J. Rock Mech. Min. Sci., 80*, pp. 325-336.
13. Seyedi, D.M., Vu, M.N., & Pouya, A. (2015). A two-scale hydromechanical model for fault zones accounting for their heterogeneous structure. *Comput. Geotech*., *68*, pp. 8-16.
14. Billaux. D. (1990). *Hydrogéologie des milieux fracturés: Géométrie, connectivité et comportement hydraulique.* Ph.D. thesis, Ecole Nationale Supérieure des Mines de Paris, in French.
15. Oda, M. (1985). Permeability tensor for discontinuous rock masses. *Géotechnique*, *35*(4), pp. 483-495.
16. Nguyen, S.T., Pham, D.C., To, Q.D., & Vu, M.N. (2016). On the effective transport properties of heterogeneous materials. *Int. J. Eng. Sci*., *104*, pp. 75-86.
17. Sævik, P. N., Berre, I., Jakobsen, M., Lien, M. (2013). A 3D computational study of effective medium methods applied to fractured media. *Transport in Porous Media*, *100*(1), pp. 115-142.
18. Vu, M. N., Nguyen, S. T., To, Q. D., & N. H. Dao. (2017). Theoretical predicting of permeability evolution in damaged rock under compressive stress. *Geophysical Journal International*, *209*(2), pp. 1352-1361.

19. Nguyen, T.T.N., Vu, M.N., Tran, N.H., Dao, N.H., & Pham, D.T. (2020). Stress induced permeability changes in brittle fractured porous rock. *International Journal of Rock Mechanics and Mining Sciences, 127,* 104224.

20. Pouya, A., & Fouché, O. (2009). Permeability of 3D discontinuity networks: New tensors from boundary-conditioned homogenisation. *Advances in Water Resources, 32*(3), pp. 303-314.

21. Pouya, A., & Vu, M.N. (2012). Numerical Modelling of Steady-State Flow in 2D Cracked Anisotropic Porous Media by Singular Integral Equations Method. *Transport Porous Med., 93*(3), pp. 475-493.

22. Louis, C. (1969). Groundwater flow in rock masses and its influence on stability. *Rock Mech. Res. Report, 10*.

23. Bai, M., & Elsworth , D. (1994). Modeling of subsidence and stress-dependent hydraulic conductivity for intact and fractured porous media. *Rock mechanics and rock engineering*, *27*(4), pp. 209-234.

24. Rutter, E. H., & Julian M. (2017). Hydraulic conductivity of bedding-parallel cracks in shale as a function of shear and normal stress. *Geological Society, London, Special Publications, 454*(1), pp. 67-84.

25. Shafiro, B., & Kachanov, M. (1997). Materials with fluid-filled pores of various shapes: effective elastic properties and fluid pressure polarization. *International Journal of Solids and Structures, 34*(27), pp. 3517-3540.

26. Nguyen, T.T.N. (2015). *Approches multi-échelles pour des maçonneries viscoélastiques.* PhD thesis. Université d'Orléans, France.

ẢNH HƯỞNG CỦA MẬT ĐỘ VẾT NỨT ĐỐI VỚI ỨNG XỬ THỦY CƠ CỦA LỖ ĐÀO NGANG CHỊU ỨNG SUẤT NÉN ĐẲNG HƯỚNG

Tóm tắt: *Việc đào lỗ thường gây phá hoại vùng lân cận của lỗ đào và do đó ảnh hưởng đến tính chất thuỷ-cơ của đất đá xung quanh. Bài báo nhắc lại các mô hình giải tích về độ thấm và các mô đun đàn hồi hiệu dụng của môi trường đá có lỗ rỗng chứa các vết nứt phân phối ngẫu nhiên. Độ thấm và các mô đun đàn hồi này là các hàm tường minh của mật độ vết nứt không thứ nguyên, tính dẫn vết nứt, chiều dài vết nứt và độ thấm môi trường. Các mô hình đề xuất này sau đó được đưa vào mã nguồn mở phần tử hữu hạn Code_Aster để nghiên cứu ứng xử kết hợp thuỷ-cơ xung quanh một lỗ đào ngang chịu ứng suất nén đẳng hướng với các trường hợp khác nhau của mật độ vết nứt. Kết quả nhận được chỉ ra rằng mật độ vết nứt làm thay đổi hệ số thấm và mô đun đàn hồi hiệu dụng và do đó dưới tác dụng của ứng suất nén đẳng hướng, mật độ vết nứt làm thay đổi đáng kể ứng xử của lỗ đào.*

Từ khóa: Hệ số thấm hiệu dụng; lỗ đào ngang; ứng xử thủy - cơ; môi trường rỗng; vết nứt.

Received: 06/4/2020; *Revised:* 21/5/2020; *Accepted for publication:* 17/6/2020

❑